MUST Journal of Research and Development (MJRD) Volume 6 Issue 3, September 2025
e ISSN 2683-6467 & p ISSN 2683-6475

Sequential Trends in Corrosion Behaviour of Surface-Ground Aluminium 7075 Thin Plates in 3.5 wt% NaCl Solution

[1]Michael Kwabena Boadu[*], [2]Anthony Agyei-Agyemang, [3]Prince Yaw Andoh and [4]Faisal Wahib Adam
[1]University for Development Studies, P.O Box TL 1882, Tamale, Ghana
[2,3,4]Kwame Nkrumah University of Science and Technology, PMB, Kumasi, Ghana
DOI: https://doi.org/10.62277/mjrd2025v6i30002

ARTICLE INFORMATION

Article History

Received: 27th July 2025
Revised: 28th August 2025
Accepted: 12th September 2025
Published: 30th September 2025

Keywords

Sequential Trends
Corrosion Behaviour
Surface-Ground
Aluminium 7075
Thin Plates

ABSTRACT

The primary aim of this study is to assess the progressive trend in the corrosion behaviour of Aluminium 7075 plates in a 3.5 wt% NaCl solution. Aluminium 7075 plates were ground using the Elliot 921 hydraulic surface grinding machine according to a factorial design schedule, and their corrosion parameters were obtained using a CorrTest Electrochemical Workstation. The electrochemical performance assessment revealed generally consistent and reproducible corrosion characteristics, albeit with some irregularities. The anodic Tafel slopes primarily fell between 64.09 and 139.54 mV, although anomalies of 291.55 mV and 366.51 mV were noted in Run Orders 46 and 48, indicating potential experimental disturbances. The cathodic slopes remained largely stable, except for unrealistic spikes of roughly 4,115,900 mV and 2,970,800 mV recorded in Run Orders 4 and 49, which likely resulted from instrumental errors. The corrosion potential initially ranged from −0.63 V to −0.58 V, stabilised between −0.67 V and −0.60 V during the mid-runs, and later shifted to values between −0.59 V and −0.67 V, illustrating the dynamics of the passive film. The current density escalated from approximately 1×10^{-5} A/cm² to around 4×10^{-5} A/cm², peaking at nearly 5×10^{-5} A/cm² in Run 27 before recovering in Run 29. The polarisation resistance decreased from above 2900 Ω·cm², exhibiting a temporary repassivation increase (3611.11 Ω·cm²) in Run 28. In summary, Aluminium 7075 demonstrated reproducible corrosion behaviour that was sensitive to surface grinding conditions.

*Corresponding author's e-mail address: boadumian@gmail.com (Boadu, M.K)

1.0 Introduction

Aluminium alloys are commonly employed in the automotive, marine, and aerospace sectors because of their light weight and adequate mechanical properties. Nonetheless, their use is significantly restricted by their resistance to corrosion (Lai *et al.,* 2022). Aluminium 7075 is used in constructing ship hulls and superstructures due to its lightweight and high strength, which contribute to fuel efficiency and increased payload capacity (Feng *et al.,* 2022).

Patel (2014) indicated that the velocity of the workpiece and the feed rate are the most important factors, as raising both parameters adversely affects surface roughness, while a higher material removal rate improves surface roughness.

Zhang *et al.* (2018) investigated how localised plastic strain affects the uneven distribution of precipitates and the corrosion behaviour of the Al–Li alloy 2A97-T6. They concluded that the Al_2CuLi phase was preferentially corroded, leading to intragranular corrosion.

Prakash *et al.* (2015) linked surface roughness to surface strain, highlighting that increased surface roughness led to greater surface activity, making corrosion more prone to occur. Furthermore, polishing the surface of the AlSi10Mg alloy to achieve a smoother finish enhanced its corrosion resistance in a 3.5% sodium chloride solution.

In contrast, Leon & Aghion (2017) found different outcomes. Their findings indicated that the corrosion resistance and fatigue life of polished Selective Laser Melting (SLM) samples were improved compared to their unpolished counterparts.

According to Goodall *et al.* (n.d.), the grinding process on the alpha-aluminium matrix creates a near-surface deformed layer that can reach a maximum thickness of 3 micrometres, consisting of ultrafine equiaxed grains with diameters ranging from 50 to 150 nanometres. This deformed layer near the surface significantly influences the alloy's corrosion behaviour; in particular, when subjected to a NaCl solution, the near-surface deformed layer undergoes preferential dissolution, which is accompanied by the formation of trenches in the aluminium matrix surrounding the eutectic silicon particles.

Niu *et al.* (2018) noted that surface machining altered the mechanical and metallurgical properties of the material in the surface layer. The impact of these alterations on corrosion behaviour varied, even for individual factors like surface roughness and work-hardening. Alvarez *et al.* (2010) asserted that a rougher surface exhibited decreased corrosion.

Corrosion behaviour is consistently associated with surface conditions (Wang *et al.,* 2017; Zhou *et al.,* 2011; Zhao & Frankel, 2007).

Burkert, *et al.* (2004) examined how grinding treatments on stainless steels influenced corrosion behaviour. They discovered that variations in grinding conditions significantly affected corrosion resistance, and different susceptibilities to corrosion could be assessed using electrochemical noise measurements.

Wang *et al.* (2018) studied the corrosion behaviour of Inconel 718 surfaces after robotic belt grinding. Their results showed a significant improvement in corrosion resistance with a reduction in abrasive particle size.

Zhou *et al.* (2018) analysed the effects of surface grinding on the corrosion behaviour of ferritic stainless steels in a boiling magnesium chloride solution. They conducted corrosion tests in this solution and found no macro-cracking on any specimen after exposure, even under high calculated applied loads.

Panadda & Hathaipat (2006) investigated the innovative use of electroplating and surface grinding techniques to enhance a coating's resistance to chemical corrosion. They found that improving the smoothness of the coating surface before plating could enhance corrosion behaviour.

The potentiodynamic polarisation (PDP) test is a method in electrochemistry that involves scanning the potential of the working electrode while measuring the resultant current density. Commonly referred to as the Tafel test, it is the most widely used electrochemical technique, complying with ASTM G 59 and ASTM F 2129 standards (Panahi *et al.,* 2024).

There is limited literature on the sequential trends in the corrosion behaviour of Aluminium 7075 plates after surface grinding. The main purpose of this research is to analyse the progressive trends in the corrosion behaviour of Aluminium 7075 plates in 3.5 wt% NaCl solution after surface grinding by utilising their polarisation curves (Tafel curves) and their trend plots.

2.0 Materials and Methods

2.1 Material

Aluminium 7075 plate was used for this research. Its elemental composition results are shown in Table 1. The corrosion parameters for the reference material

are also shown in Table 2. The density was found to be 2.77 g/cm^3, and the equivalent mass was found to be 9.0 g/equiv. The Stern-Geary coefficient is chosen to be 26.0 mV.

2.2 Design of Experiment

A factorial design was used to conduct the experiment. A total of 54 runs were obtained because the experimental runs were replicated. The factorial design is shown in Table 3 with the low (0), medium (1) and high (2) levels utilised during the experiment. The detailed experimental design with levels and runs is shown in Table 4. The geometrical representation of a factorial design is shown in Figure 1. The numbers denote the experimental runs.

Figure 1

Geometrical Representation of 3^3 Factorial Design (Nikolaos et al., 2015)

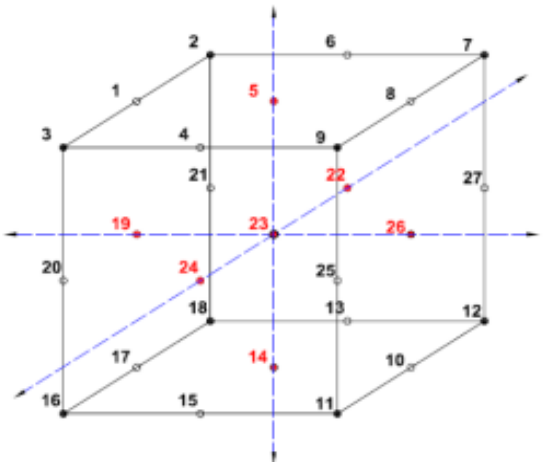

2.3 Preparation of Samples for Corrosion Analysis Test

A total of 54 samples were used for the corrosion analysis test. The samples were cut from the parent plate using a 750 W Total Angle Grinder with a no-load speed of 12000 rpm and a rated voltage of 220-240 V. The total length of each specimen was 50 mm. The width was 20 mm. The plate thicknesses were 3.8 mm, 3.5 mm, and 3.0 mm. The samples were not polished since their surfaces were altered by the surface grinding process; they were also fresh samples with mirrored surfaces. The samples were labelled CR 1 to CR 54. Figure 2 shows the specimen geometry obtained after preparation.

Figure 2

Geometry of Samples after Preparation

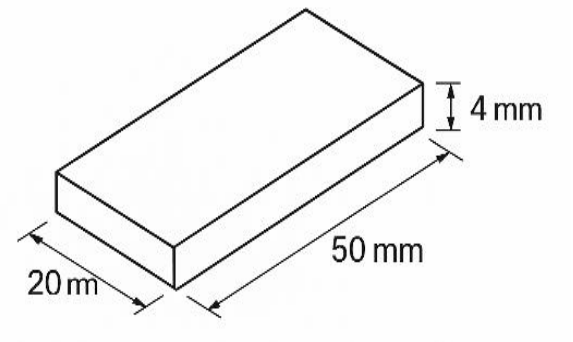

Table 1

Chemical Composition of Aluminium 7075 (B209, 2014)

Element	Si	Fe	Zn	Mg	Ti	Cu	Cr	Mn	Pb	Al
% by Weight	≤ 0.40	≤ 0.50	5.1- 6.1	2.1– 2.9	≤0.20	1.2-2.0	0.18-0.28	≤ 0.3	≤ 0.05	≥ 89.97

Table 2

Electrochemical Properties of Aluminium 7075

Variables	Low (0)	Medium (1)	High (2)
Table Speed (spm)	2.0	15.0	50.0
Feed (mm)	1.0	2.0	5.0
Grinding Depth (mm)	0.2	0.5	1.0

Table 3

The 3^3 Experimental Design Levels

Ecorr (V)	Icorr A/cm^2	ba mV	bc mV	Rp Ω.cm^2	CR mm/a
-0.644	0.000025	97.54	27373.87	1048.26	0.27

Table 4

Detailed Experimental Design with Levels and Runs

Runs	V_s spm	f mm	d mm	Runs	V_s spm	f mm	d mm
1	2.0	1.0	0.2	28	2.0	1.0	0.2
2	15.0	1.0	0.2	29	15.0	1.0	0.2
3	50.0	1.0	0.2	30	50.0	1.0	0.2
4	2.0	2.0	0.2	31	2.0	2.0	0.2
5	15.0	2.0	0.2	32	15.0	2.0	0.2
6	50.0	2.0	0.2	33	50.0	2.0	0.2
7	2.0	5.0	0.2	34	2.0	5.0	0.2
8	15.0	5.0	0.2	35	15.0	5.0	0.2
9	50.0	5.0	0.2	36	50.0	5.0	0.2
10	2.0	1.0	0.5	37	2.0	1.0	0.5
11	15.0	1.0	0.5	38	15.0	1.0	0.5
12	50.0	1.0	0.5	39	50.0	1.0	0.5
13	2.0	2.0	0.5	40	2.0	2.0	0.5
14	15.0	2.0	0.5	41	15.0	2.0	0.5
15	50.0	2.0	0.5	42	50.0	2.0	0.5
16	2.0	5.0	0.5	43	2.0	5.0	0.5
17	15.0	5.0	0.5	44	15.0	5.0	0.5
18	50.0	5.0	0.5	45	50.0	5.0	0.5
19	2.0	1.0	1.0	46	2.0	1.0	1.0
20	15.0	1.0	1.0	47	15.0	1.0	1.0
21	50.0	1.0	1.0	48	50.0	1.0	1.0
22	2.0	2.0	1.0	49	2.0	2.0	1.0
23	15.0	2.0	1.0	50	15.0	2.0	1.0
24	50.0	2.0	1.0	51	50.0	2.0	1.0
25	2.0	5.0	1.0	52	2.0	5.0	1.0
26	15.0	5.0	1.0	53	15.0	5.0	1.0
27	50.0	5.0	1.0	54	50.0	5.0	1.0

2.4 Experimental Procedure

The samples were ground using the Elliot 921 Hydraulic Grinding Machine with respect to the Design of Experiment schedule. The plate's thicknesses of 3.8 mm, 3.5 mm, and 3.0 mm were achieved after the surface grinding operation. The potentiodynamic polarisation test, which uses a CorrTest electrochemical workstation, was employed to evaluate the corrosion behaviour of the aluminium 7075 thin plates after the surface grinding operation. Figure 3 shows the experimental set-up. Samples of Aluminium 7075 thin plates with an exposed ground surface area of 10 cm^2 were used. The other surfaces, including the edges and the unground surface, were coated with epoxy. The experiment was conducted in deaerated 3.5 wt.% NaCl solution at room temperature (25°). The specimen was polarised from -250.0 mV (OCP) to +250.0 mV (OCP), with the scanning rate of 0.5 mV/s. The Ag/AgCl reference electrode was used. A graphite rod was also used as a counter electrode. The Aluminium 7075 thin plates were utilised as a working electrode. The data was obtained utilising the CS Studio6 software. The fit auto Tafel option was used to generate the corrosion data for all the runs except in Run 7, where it failed. In this case, the fit auto Tafel between cursors was employed. The polarisation resistance ( ) was calculated from the known Stern-Geary coefficient (26.0 mV) and the corrosion current density (Icorr) results for the various samples.

Figure 3

Experimental Set-up for the Corrosion Test

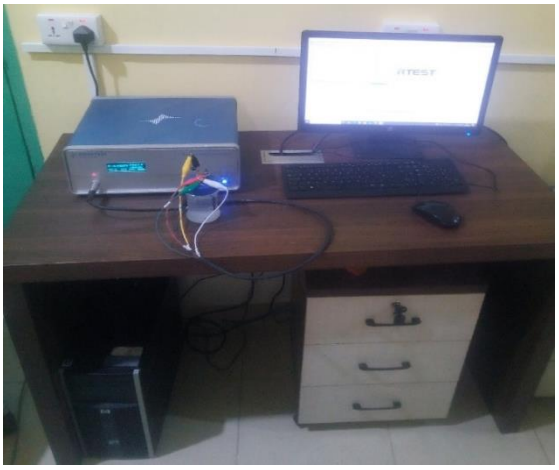

4.0 Results and Discussion

The graph for the variation of the anodic Tafel slope and the cathodic Tafel slope with respect to the experimental runs, or run order, is presented in Figures 4 and 5, respectively.

Figure 4 shows a stable trend in anodic Tafel slope readings throughout the majority of the sample, interrupted by a notable spike in signal intensity between the samples in run orders 46 and 48. At first, the anodic Tafel slope signal varies moderately within a range of approximately 60–130 mV, indicating a fairly steady baseline response during the early to mid-phase of the experimental runs. Minor peaks, such as those occurring around the samples in run orders 13 and 26, may represent temporary disturbances or slight alterations in sample properties or instrument sensitivity. However, a significant anomaly appears in Samples of Run Orders 46 and 48, where the anodic Tafel slope readings jump sharply to 291.55 mV and 366.51 mV, respectively. These significant spikes point to the possibility of contamination, sudden matrix variations, or the introduction of a high-

concentration anodic slope source. Such sudden deviations from the otherwise stable trend strongly indicate that these data points do not represent the usual system behaviour and may require additional investigation or exclusion from specific analyses. After these peaks, the readings swiftly return to baseline levels of about 80–140 mV, with some remaining fluctuations potentially indicating system recovery or carryover effects. In conclusion, while the overall dataset reflects a consistent and reproducible signal in most of the samples, the brief yet extreme outliers at the end of the sequence underscore the importance of thoroughly examining anomalous occurrences that could disrupt analytical continuity.

From Figure 5, the samples in Run Orders 4 and 49 were excluded because they showed a remarkable spike in cathodic Tafel slopes at 4,115,900 mV and 2,970,800 mV, respectively. Throughout most of the experiment, the cathodic Tafel slope remains mostly stable, suggesting minimal fluctuations in cathodic kinetics during those runs. The sudden, extreme surge of the samples in run orders 4 and 49 appears to be an outlier and is likely due to a measurement mistake, instrument malfunction, or data recording problem. Such an anomaly is inconsistent with the steady electrochemical behaviour noticed in the previous runs and, as such, should be considered an exception. If this peculiar value is excluded, the overarching trend indicates that the cathodic reaction mechanisms showed consistency across the experiment, reflecting stable corrosion kinetics and surface conditions, thereby further validating the grinding and testing procedures utilised.

Figure 6's graph illustrates the corrosion potential (Ecorr) against the sequence of runs, with a noticeable general pattern of fluctuating instability interspersed with moments of stabilisation throughout the experimental process. During the initial runs (approximately the first five), the Ecorr values of the samples fluctuate sharply between about –0.63 V and –0.58 V, indicating an unstable electrochemical interface likely related to early surface activity or incomplete formation of the passive film. As the sequence progresses into the mid-runs (around run orders 10–35), the corrosion potential of the samples narrows to a range between –0.67 V and –0.60 V, suggesting partial stabilisation; however, recurring spikes and drops may represent localised corrosion events or the inconsistent effects of grinding-induced surface conditions. In the later runs (beyond run order 40), the trend remains variable, with values alternating between less negative readings (approximately –0.59 V) and more negative ones (near –0.67 V), indicating a dynamic competition between the reinforcement and breakdown of the passive film. Overall, the ongoing fluctuations underscore Aluminium 7075's electrochemical behaviour sensitivity to surface preparation and highlight the reproducibility challenges associated with grinding-altered surfaces.

The graph, depicted in Figure 7, illustrates a trend of increasing corrosion current density (Icorr) against run order, with noticeable transient fluctuations occurring around the midpoint of the runs. In the initial phase (up to about run order 20), Icorr values for the samples gradually increased from approximately 0.00001 A/cm² to about 0.00002 A/cm², suggesting a progressive rise in corrosion activity, possibly due to changes in surface reactivity or the gradual degradation of protective layers. A significant spike occurs at the sample in run order 27, where Icorr reaches a peak of nearly 0.00005 A/cm², subsequently followed by a sharp drop to its lowest point of roughly 0.000007 A/cm² at run order 28. This sudden change indicates a rapid instability or failure of the passive film, which is promptly followed by a swift repassivation or reconditioning of the surface. After this instance, the current density begins to increase gradually again, reaching approximately 0.00004 A/cm² by Run Order 54. In summary, the figure reveals that while the corrosion behaviour of Aluminium 7075 thin plate tends to intensify through successive runs, transient surface events like film breakdown and renewal introduce fluctuations into the electrochemical response, demonstrating the sensitivity of the alloy's surface to run order.

The plotted values of polarisation resistance (Rp) against run order, in Figure 8, show a primarily decreasing trend with a marked interruption at the halfway point of the sequence. The Rp value of the sample at Run 1 was quite high, exceeding 2900 Ω·cm², but it steadily declined with each run,

indicating a gradual alteration in surface or interfacial conditions—probably due to ongoing surface modification, film breakdown, or loss of passivity. An unexpected and notable spike occurs at the sample in run order 28, where the resistance suddenly peaks above 3600 Ω·cm², disrupting the otherwise consistent decline. This singular increase likely indicates a sudden, temporary repassivation event, an experimental reset, or potential contamination that momentarily raised the interfacial resistance. Following this peak, resistance decreases again and continues on a similar downward path, reflecting the trend seen prior to the disturbance. This symmetrical pattern before and after the spike indicates that the system returned to its previous electrochemical state after the transient occurrence. In summary, the data suggests that the system experiences a continual reduction in polarisation resistance over the course of multiple runs, potentially due to persistent electrochemical exposure, punctuated only by this one significant anomaly. Identifying the reason behind this mid-sequence spike is critical to preserving the reliability and interpretability of long-term Rp measurements.

Figure 4

A Graph of Anodic Tafel slope (ba) against Run Order

Figure 5

A Graph of Cathodic Tafel slope (bc) against Run Order

Figure 6

A Graph of Corrosion Potential (Ecorr) versus Run Order

Figure 7

A Graph of Corrosion Current Density (Icorr) versus Run Order

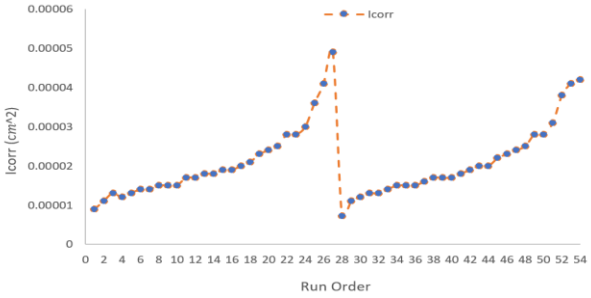

Figure 8

A Graph of Polarization Resistance (Rp) versus Run Order

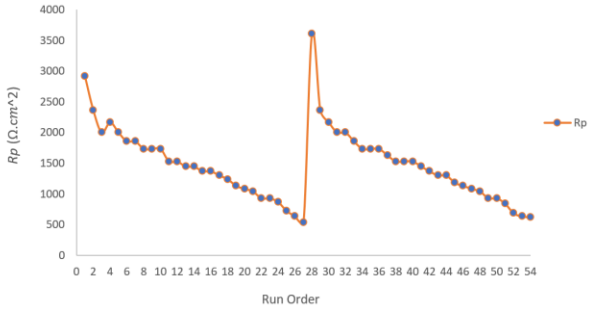

The Tafel plots are illustrated in Figures 9 through 19. As depicted in Figure 9, the samples in Runs 1 through 5 displayed closely aligned patterns, illustrating the reproducibility of the electrochemical properties of Aluminium 7075 in NaCl solution. The corrosion potential (Ecorr) for all samples was approximately −0.6 V, with minimal variations among the curves, indicating the alloy's stability under the testing conditions. The samples in runs 1, 2, and 3 showed almost identical characteristics in both cathodic and anodic branches, featuring smooth polarisation responses, while the sample in run 4 presented slightly more variability in the cathodic region, hinting at minor

surface instabilities or experimental noise. The sample in Run 5 exhibited a behaviour that was quite similar to that of the samples in Runs 1–3, further reinforcing the consistency of the measurements. In every instance, the cathodic branches indicated a gradual reduction process, while the anodic branches reflected an increase in current density linked to the dissolution of active metal. The uniformity of the curves among the samples emphasises the dependability of the experimental method and supports the corrosion trends observed for Aluminium 7075 thin plate.

From Figure 10, the samples in runs 6 to 10 show very similar electrochemical responses, indicating the electrochemical corrosion behaviour of Aluminium 7075 in NaCl electrolyte is reproducible. The corrosion potential (Ecorr) for each sample ranges from −0.65 to −0.60 V, with slight variations, implying the alloy retains a stable corrosion potential throughout the repeated tests. The cathodic branches of the samples in runs 6, 7, and 8 largely align, reflecting consistency in the reduction reactions, while the samples in runs 9 and 10 present a bit more variability but still follow the same overall trend. On the anodic side, all samples show the typical increase in current density associated with active dissolution, with minimal differences among the curves. The close clustering of the samples emphasises the reliability of the electrochemical testing method and confirms the consistency of the corrosion characteristics. Overall, the findings suggest that the alloy demonstrates stable corrosion behaviour, with negligible effects of experimental conditions on multiple runs.

From Figure 11, the samples in Runs 11 to 15 demonstrate robust reproducibility, with all samples revealing comparable electrochemical behaviour of Aluminium 7075 in NaCl solution. The corrosion potential (Ecorr) is consistently found around −0.6 V, showing only minor variations among the samples. The samples in runs 12, 13, 14, and 15 exhibit nearly identical anodic and cathodic trends, whereas the sample in run 11 presents a slightly greater variability in the cathodic part, which may be attributed to differences in surface condition or measurement noise. Nevertheless, the overall polarisation response remains consistent across all runs. The anodic branches show a gradual increase in current density, signifying the active dissolution of the alloy, while the cathodic branches display a consistent reduction trend. The close alignment of the samples reinforces the reliability and stability of the corrosion process, validating the high reproducibility of the alloy's electrochemical response across various measurements.

The Tafel polarisation curves of the samples in runs 16 to 20 displayed in Figure 12 demonstrate significant reproducibility, with all samples reflecting a similar electrochemical response in the NaCl solution. The corrosion potential (Ecorr) is consistently measured at approximately −0.6 V, with only minor discrepancies observed between the samples. The samples in runs 18, 19, and 20 exhibit nearly identical trends in both the cathodic and anodic regions, suggesting consistent corrosion characteristics, whereas the samples in runs 16 and 17 display slightly more variation in the cathodic branch, potentially attributable to differences in surface conditions or experimental noise. Nonetheless, the overall polarisation behaviour is stable across all samples. The anodic branches exhibit a consistent increase in current density, indicating the active dissolution of the alloy, while the cathodic branches show a steady reduction trend. The close alignment of the curves reinforces the stability and reproducibility of the corrosion process, supporting the dependability of the material's electrochemical response under the tested conditions.

From Figure 13, the samples in runs 21 through 25 indicate exceptional reproducibility, with each sample demonstrating similar electrochemical behaviour in the NaCl solution. The corrosion potential (Ecorr) is consistently around −0.6 V, showing only slight variations among the measurements. The samples in runs 21, 22, 23, and 24 display nearly identical cathodic and anodic branches, which indicates stable and uniform corrosion behaviour. The sample in Run 25 exhibits a bit more variation in the cathodic region, potentially due to variations in surface conditions or minor inconsistencies in the experimental setup. However, this deviation is minimal and does not affect the overall analysis. The anodic branches across all runs show a gradual and consistent increase in current density, signifying the active

dissolution of the alloy, while the cathodic branches present a steady reduction trend. The close grouping of the polarisation curves underscores the stability and repeatability of the corrosion response, bolstering the credibility of the electrochemical measurements and the consistent performance of the material under the specified testing conditions.

The Tafel polarisation curves for the samples in runs 26 to 30 shown in Figure 14 demonstrate strong reproducibility, with all tests exhibiting comparable electrochemical behaviour of the material analysed in the NaCl solution. The corrosion potential (Ecorr) consistently hovers around −0.6 V, showing slight fluctuations among the individual tests. The samples in runs 26, 27, and 28 reveal nearly overlapping cathodic and anodic branches, which indicate stable corrosion characteristics. In contrast, the samples in runs 29 and 30 display a bit more divergence, especially in the anodic region, where they reveal minimal current densities—potentially indicating enhanced surface reactivity or minor variations in surface conditions. Nonetheless, the cathodic branches remain closely aligned across all tests, highlighting a uniform reduction process. The anodic branches generally show a continual increase in current density, confirming active dissolution behaviour. In summary, the curves demonstrate dependable electrochemical performance with slight deviations, reinforcing the stability and repeatability of the material's corrosion response under the examined conditions.

From Figure 15, the Tafel polarisation curves illustrate strong reproducibility, with all experiments revealing consistent electrochemical characteristics of the investigated material in the NaCl solution. The corrosion potential (Ecorr) tends to stay clustered around −0.6 V, showing minimal variation between the runs. The samples in runs 31, 32, 33 and 35 present almost identical cathodic and anodic branches, indicating uniform corrosion behaviour and a stable electrochemical response. The sample in Run 34, on the other hand, displays a slightly greater deviation in the cathodic branch, with higher current densities at more negative potentials, potentially due to localised surface variations or differences in passivation behaviour. Nonetheless, the cathodic branches across all runs align closely, implying a consistent reduction mechanism. The anodic branches show a gradual increase in current density, typical of active dissolution. Overall, the close clustering of the curves supports the reliability of the measurements and confirms the consistency of the corrosion response under the specified test conditions.

The Tafel curve for the samples in runs 36 to 40, shown in Figure 16, exhibits remarkable reproducibility and consistently similar electrochemical behaviour in NaCl solution. The corrosion potential (Ecorr) is consistently clustered around −0.6 V, indicating very little variation among the samples. Each of the five samples in each run presents nearly identical cathodic branches, with overlapping data extending to extremely low current densities, suggesting a stable and uniform cathodic reduction process. The anodic branches also display a closely aligned trend, with a gradual increase in current density as the potential becomes more positive, indicating active dissolution of the alloy. Some minor differences are noted in the very low current density region of the sample in Run 40, where a slightly elongated horizontal section appears, likely attributed to experimental noise or transient surface passivation effects; however, this does not substantially impact the overall consistency. The closely grouped anodic and cathodic curves further validate the high reproducibility of the corrosion response and reinforce the material's reliable electrochemical behaviour across the runs.

The Tafel polarisation curves for the samples in runs 41 through 45, displayed in Figure 17, demonstrate strong reproducibility, as all samples show comparable electrochemical behaviour of the examined material in the NaCl solution. The corrosion potential (Ecorr) consistently hovers around −0.6 V, exhibiting only minor fluctuations among the samples. The samples in runs 43, 44, and 45 reveal nearly overlapping cathodic and anodic branches, which suggest stable and repeatable corrosion behaviour. The sample in runs 41 and 42 presents slightly more variation, especially in the cathodic area, where discrepancies may result from differences in surface conditions or transient effects during the measurements. Nonetheless, the overall cathodic trend remains stable, indicating a uniform reduction process. The anodic branches for all runs

demonstrate a gradual increase in current density as the potential rises, aligning with active material dissolution. All in all, the samples exhibit a significant degree of overlap, reinforcing the reliability and consistency of the electrochemical response under the tested conditions, with only slight variability noted in the cathodic regions of a few samples.

The Tafel curve for the sample in runs 46 to 50 in Figure 18 shows significant variability, suggesting reduced reproducibility compared to earlier sets. While the corrosion potential (Ecorr) typically hovers around −0.6 V, the variation in both the cathodic and anodic branches indicates inconsistencies in the electrochemical behaviour among the samples. The samples in runs 47 and 48 exhibit a somewhat similar pattern, particularly in the cathodic area, although there are slight deviations. Conversely, the sample in Run 46 has a considerably high anodic Tafel slope, which may imply increased dissolution activity or possible surface activation. The sample in Run 49 has comparatively an extremely higher cathodic branch, indicating a high reduction process. The sample in Run 50 also demonstrates some variation, especially in the cathodic branch, with increased scatter likely attributed to surface imperfections or experimental noise. The anodic branches, in general, reveal different slopes and current densities, highlighting inconsistencies in corrosion kinetics. This variability in the data implies that external elements—like surface preparation or instrument fluctuations—may have impacted the outcomes. Consequently, the reproducibility of the corrosion response in this series is moderate.

The Tafel curve for the samples in runs 51 to 54, in Figure 19, shows reasonably good reproducibility, indicating a similar electrochemical performance of the tested material in the NaCl solution. The corrosion potential (Ecorr) hovers around −0.6 V for all samples, signifying a comparable start to corrosion. However, there are notable differences in both the cathodic and anodic sections. The samples in runs 52 and 53 present closely matched curves in both areas, indicating a stable corrosion response. Conversely, the sample in Run 51 displays a more significant divergence in the anodic section, with a lower current density that may suggest less localised activation or slight changes in surface condition. The sample in Run 54 reveals more variability in the cathodic section, possibly due to noise or uneven surface characteristics. Despite these discrepancies, the overall patterns remain similar, with all curves indicating active dissolution in the anodic section and a consistent reduction process in the cathodic section. Although not as closely grouped as the most reproducible datasets, this information still indicates generally dependable electrochemical behaviour, with some variability between the experimental runs.

Figure 9

Tafel Plot for Run 1 - Run 5

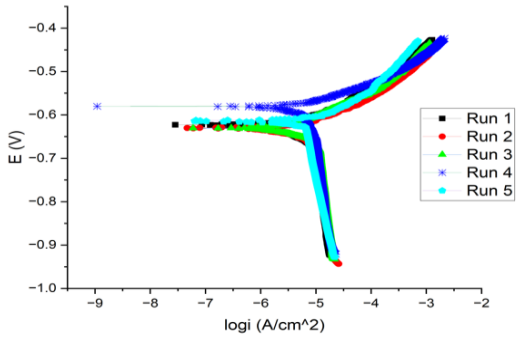

Figure 10

Tafel Plot for Run 6 - Run 10

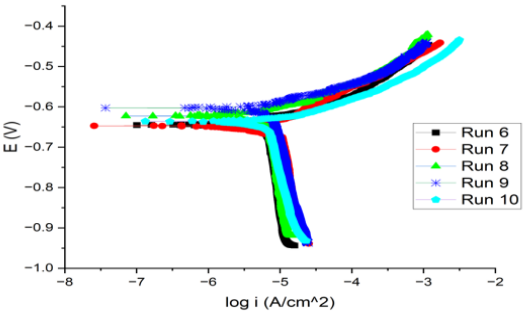

Figure 11

Tafel Plot for Run 11 – Run 15

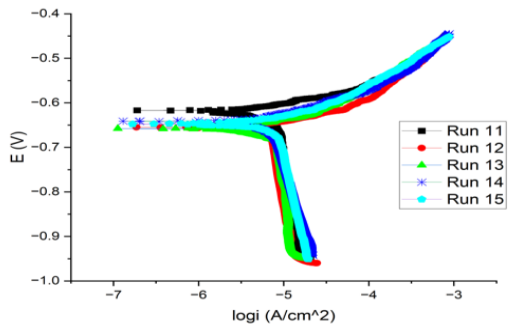

Figure 12
Tafel Plot for Run 16 – Run 20

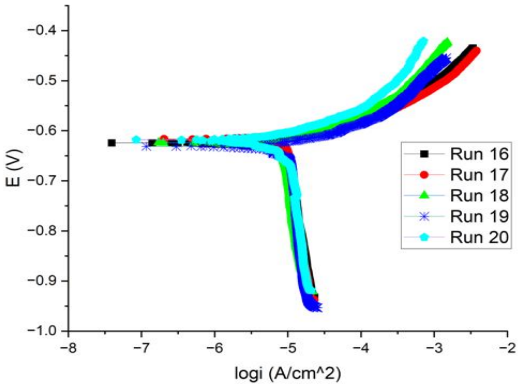

Figure 13
Tafel Plot for Run 21 – Run 25

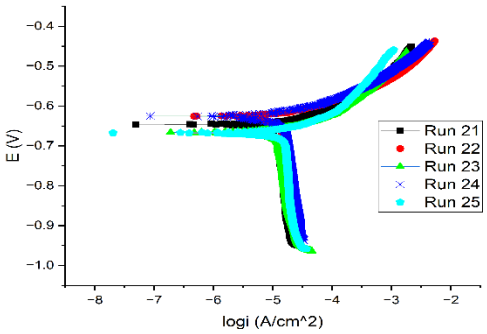

Figure 14
Tafel Plot for Run 26 – Run 30

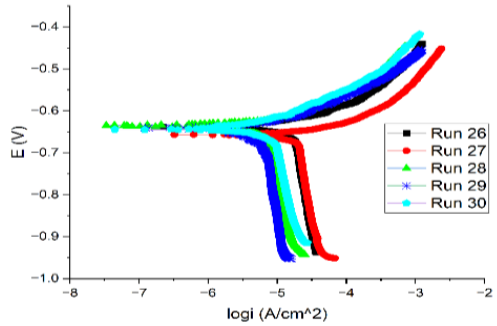

Figure 15
Tafel Plot for Run 31 – Run 35

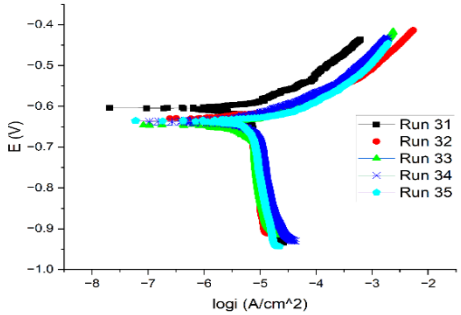

Figure 16
Tafel Plot for Run 36 – Run 40

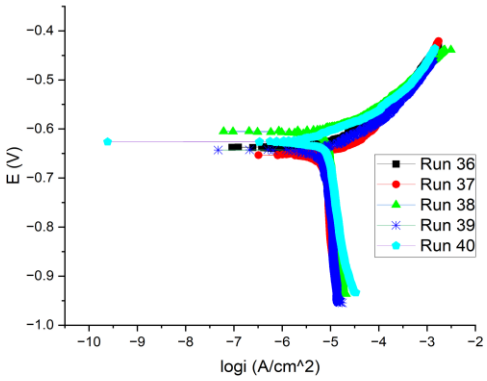

Figure 17
Tafel Plot for Run 41 – Run 45

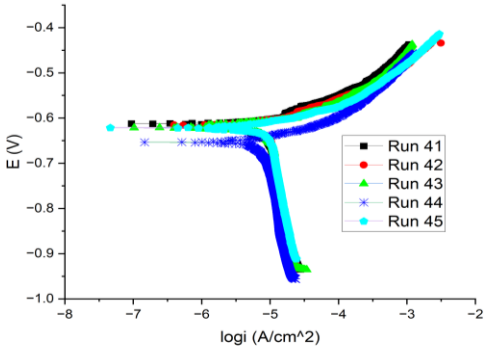

Figure 18
Tafel Plot for Run 46 – Run 50

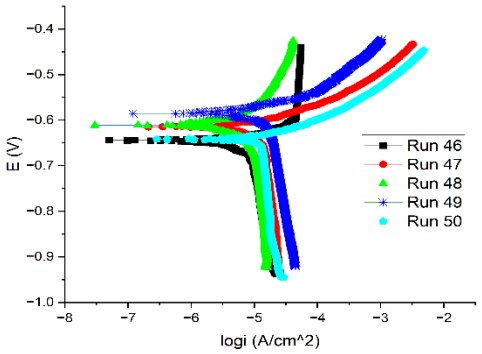

Figure 19
Tafel Plot for Run 51 – Run 54

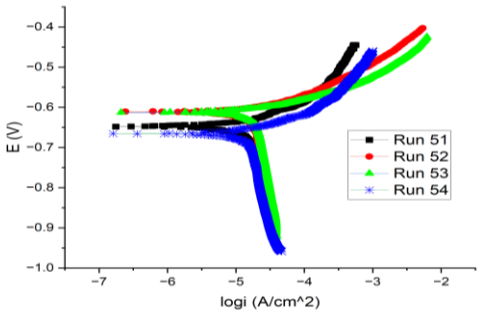

5.0 Conclusions

The electrochemical assessment of Aluminium 7075 thin plates across several runs shows a largely consistent and repeatable corrosion behaviour, although some anomalies were observed. The anodic Tafel slopes primarily fell within the range of 64.09–139.54 mV, but extreme outliers of 291.55 mV and 366.51 mV were noted during Run Orders 46 and 48, respectively, suggesting potential contamination or disruptions in the experiment. The cathodic Tafel slopes also exhibited relative stability, with unrealistic spikes of approximately 4,115,900 mV and 2,970,800 mV occurring at Run Orders 4 and 49, indicating possible errors in measurement or instrumentation. Initially, the corrosion potential varied between −0.63 V and −0.58 V, then stabilised within a narrower range of −0.67 V to −0.60 V during the mid-runs; however, it later fluctuated again between −0.59 V and −0.67 V, reflecting an ongoing competition between passive film formation and deterioration. The corrosion current density showed an upward trend from roughly 1×10^{-5} A/cm² at the beginning, reaching about 4×10^{-5} A/cm² by Run Order 54, with a pronounced peak of nearly 5×10^{-5} A/cm² at Run 27, followed by a drop to around 7×10^{-6} A/cm² at Run 28, illustrating transient film failure and swift recovery. Polarisation resistance started above 2900 Ω·cm² but consistently declined with increasing run order, aside from a spike to 3611.11 Ω·cm² at Run 28, indicating a temporary event of re-passivation before the downward trend continued. Together, these results reaffirm that, while the AA7075 thin plate demonstrates generally reproducible corrosion characteristics, its response is highly sensitive to changes in surface conditions, with increasing corrosion current density and decreasing resistance pointing to ongoing surface degradation and momentary anomalies highlighting the intricate dynamics between passive film breakdown and renewal.

6.0 Funding Declaration

This research received no specific grant from any funding agency in the public, commercial, or not-for-profit sectors.

7.0 Competing Interest

The authors state that their known financial conflicts or interpersonal connections did not impact the work presented in this paper.

8.0 Conflict of Interest

We declare no conflict of interest.

9.0 Ethical Statement

This material is the authors' own original work, which has not been previously published elsewhere.

10.0 References

Alvarez, R. B., Martin, H. J., Horstemeyer, M. F., Chandler, M. Q., Williams, N., Wang, P. T., & Ruiz, A. (2010). Corrosion relationships as a function of time and surface roughness on a structural AE44 magnesium alloy. *Corrosion Science, 52*(5), 1635-1648. https://doi.org/10.1016/j.corsci.2010.01.017

ASTM B209. (2014). *Standard specification for aluminum and aluminum-alloy sheet and plate.* American Society for Testing and Materials.

Burkert, A., Schilling, K., & Heyn, A. (2004). The influence of grinding treatment of stainless steels on the corrosion behaviour. *Materials and Corrosion, 55* (10), 787-793. https://doi.org/10.1002/maco.200403767

Feng, Z. B., Li, J., Ma, J.-C., Su, Y., Zhang, X., Mao, Y., & Zhao, Z. (2022). EBSD characterization of 7075 aluminum alloy and its corrosion behaviors in SRB marine environment. *Journal of Marine Science and Engineering, 10* (6), 740. https://doi.org/10.3390/jmse10060740

Goodall, M. D., Pawar, S., Curioni, M., Morsch, S., Unthank, M. G., Gibbon, S. R., & Zhou, X. (n.d.). The influence of mechanical grinding on the microstructure and corrosion behaviour of A356 aluminium alloys. *Unpublished manuscript.*

Lai, H. S., Jiang, X., Li, H., Cui, H., Zhao, Z., Guo, H., & Li, L. (2022). Investigation of 7075 aluminum alloy corrosion in marine environment. *International Journal of Electrochemical Science, 17*(5), 220559. https://doi.org/10.20964/220559

Leon, A., & Aghion, E. (2017). Effect of surface roughness on corrosion fatigue performance of

AlSi10Mg alloy produced by selective laser melting (SLM). *Materials Characterization, 131*, 188-194. https://doi.org/10.1016/j.matchar.2017.06.020

Nikolaos, M. V., Fountas, N. A., Koraidis, C., Koutsomichalis, A., & Psyllaki, P. (2015). Modeling of surface finish in turning of a brass alloy based upon statistical multi-parameter analysis. *Tribological Journal BULTRIB, 5*, 303–313. [Conference paper]

Niu, J., Wang, Q., Wang, Q., Hua, Y., & Wang, G. (2018). Effect of machining-induced surface integrity on the corrosion behavior of Al–Li alloy 2A97 in sodium chloride solution. *Materials and Corrosion, 70* (2), 259-267. https://doi.org/10.1002/maco.201810024

Panadda, N., & Hathaipat, K. (2006). Improved corrosion resistance of thermally sprayed coating via surface grinding and electroplating techniques. *Surface and Coatings Technology, 201*(3-4), 737-743. https://doi.org/10.1016/j.surfcoat.2005.12.007

Panahi, P., Nouri Khorasani, S., Mensah, R. A., Das, O., & Esmaeely Neisiany, R. (2024). A review of the characterization methods for self-healing assessment in polymeric coatings. *Progress in Organic Coatings, 186*, 108055. https://doi.org/10.1016/j.porgcoat.2024.108055

Patel, S. (2014). An experimental investigation on cylindrical grinding process parameters for EN8 using regression analysis. *International Journal of Engineering Development and Research, 2*(2), 2486–2491.*

Prakash, M., Moon, A. P., Mondal, K., & Shekhar, S. (2015). Effect of machining configurations on the electrochemical response of mild steel in 3.5% NaCl solution. *Journal of Materials Engineering and Performance, 24* (10), 3643–3650. https://doi.org/10.1007/s11665-015-1667-2

Wang, J. W., et al. (2018). An investigation of surface corrosion behavior of Inconel 718 after robotic belt grinding. *Materials, 11*(12), 2440. https://doi.org/10.3390/ma11122440

Wang, S. S., Yang, F., & Frankel, G. S. (2017). Effect of altered surface layer on localized corrosion of aluminum alloy 2024. *Journal of The Electrochemical Society, 164*(6), C317–C326. https://doi.org/10.1149/2.0121706jes

Zhang, X., Zhou, X., Hashimoto, T., Liu, B., Luo, C., Sun, Z., & Ma, Y. (2018). Corrosion behaviour of 2A97-T6 Al-Cu-Li alloy: The influence of non-uniform precipitation. *Corrosion Science, 132*, 1-8. https://doi.org/10.1016/j.corsci.2017.12.010

Zhao, Z., & Frankel, G. S. (2007). On the first breakdown in AA7075-T6. *Corrosion Science, 49* (7), 3064-3088. https://doi.org/10.1016/j.corsci.2007.02.004

Zhou, N., Pettersson, R., Schönning, M., & Peng, R. L. (2018). Influence of surface grinding on corrosion behavior of ferritic stainless steels in boiling magnesium chloride solution. *Materials and Corrosion, 69*(11), 1560–1571. https://doi.org/10.1002/maco.201810401

Zhou, X., Liu, Y., Thompson, G. E., Scamans, G. M., Skeldon, P., & Hunter, J. A. (2011). Near-surface deformed layers on rolled aluminum alloys. *Metallurgical and Materials Transactions A, 42* (5), 1373-1385. https://doi.org/10.1007/s11661-010-0466-2